IV

ELECTRICAL ENGINEERING

N66-18067

(ACCESSION NUMBER)	(THRU)
14	1
(PAGES)	(CODE)
CR 70528	07
(NASA CR OR TMX OR AD NUMBER)	(CATEGORY)

FACILITY FORM 602

Hard copy (HC) $3.00

Microfiche (MF) .50

ff 653 July 65

AUBURN RESEARCH FOUNDATION

AUBURN UNIVERSITY

AUBURN, ALABAMA

NASA CR70528

TECHNICAL REPORT NUMBER 2

THE DESIGN, CONSTRUCTION AND EVALUATION OF AN ELLIPTICALLY POLARIZED ANTENNA ELEMENT

PREPARED BY

ANTENNA RESEARCH LABORATORY

E. R. GRAF, TECHNICAL DIRECTOR

December 18, 1964

CONTRACT NAS8-11251

GEORGE C. MARSHALL SPACE FLIGHT CENTER

NATIONAL AERONAUTICS AND SPACE ADMINISTRATION

HUNTSVILLE, ALABAMA

APPROVED BY

C. H. Weaver
Head Professor
Electrical Engineering

SUBMITTED BY

H. M. Summer
Project Leader

TECHNICAL REPORT NUMBER 2

THE DESIGN, CONSTRUCTION AND EVALUATION OF AN ELLIPTICALLY POLARIZED ANTENNA ELEMENT

PREPARED BY

ANTENNA RESEARCH LABORATORY

E. R. GRAF, TECHNICAL DIRECTOR

December 18, 1964

CONTRACT NAS8-11251

GEORGE C. MARSHALL SPACE FLIGHT CENTER

NATIONAL AERONAUTICS AND SPACE ADMINISTRATION

HUNTSVILLE, ALABAMA

APPROVED BY

C. H. Weaver
Head Professor
Electrical Engineering

SUBMITTED BY

H. M. Summer
Project Leader

PREFACE

A theoretical discussion of the electromagnetic field characteristics of the electric-magnetic dipole is presented. It is shown that the radiation field vector is, in general, elliptically polarized, and that under certain conditions circular polarization is possible at every point in space. A description of the techniques used to construct the antenna is then given, followed by an evaluation of the experimentally obtained radiation field patterns.

TABLE OF CONTENTS

I. INTRODUCTION..... 1

II. THEORETICAL DISCUSSION..... 2

The Radiation Field of a Thin Linear Antenna

The Radiation Field of a Loop Antenna

The Effect of the Combined Fields

III. CONSTRUCTION OF ANTENNA..... 16

Description of Antenna

Description of Baluns

Input Impedance

Impedance Matching

IV. EVALUATION OF ANTENNA PERFORMANCE..... 20

Comparison of Theoretical and Experimental Patterns

BIBLIOGRAPHY..... 22

APPENDIX A..... 23

APPENDIX B..... 27

LIST OF FIGURES

1. The Coordinate System Showing Antenna Orientation..... 3

2. The Figure for the Derivation of the Field of a Thin-Linear Antenna..... 4

3. The Figure for the Derivation of the Field of a Loop Antenna..... 9

4. A Photograph of the Electric-Magnetic Dipole Antenna.... 17

5. A Block Diagram of the Impedance Measuring System..... 19

A-1. The Radiation Field of a Half-Wave Center-Fed Thin Linear Dipole..... 24

A-2. The Radiation Field of a Loop Antenna With Uniform Current Distribution..... 25

A-3. The Theoretical Azimuth Pattern of a Loop or a Dipole... 26

B-1. The Azimuth Pattern of the Dipole..... 28

B-2. The Azimuth Pattern of the Loop..... 29

B-3. The Polarization Pattern of the Antenna, Vertically Polarized Signal..... 30

B-4. The Polarization Pattern of Antenna, Horizontally Polarized Signal..... 31

B-5. A Conical Cut of the Antenna, $\theta = 90^{o}$..... 32

B-6. A Conical Cut of the Antenna, $\theta = 85^{o}$..... 33

B-7. A Conical Cut of the Antenna, $\theta = 80^{o}$..... 34

B-8. A Conical Cut of the Antenna, $\theta = 75^{o}$..... 35

B-9. A Conical Cut of the Antenna, $\theta = 70^{o}$..... 36

B-10. A Conical Cut of the Antenna, $\theta = 65^{\circ}$..... 37

B-11. A Conical Cut of the Antenna, $\theta = 60^{\circ}$..... 38

THE DESIGN, CONSTRUCTION AND EVALUATION OF AN ELLIPTICALLY POLARIZED ANTENNA ELEMENT

S. B. Roberts and E. R. Graf

I. INTRODUCTION

The purpose of this study was to design, construct and evaluate an elliptically polarized 137 megacycle antenna to be used as an element in a radio direction finder. Elliptical polarization of the element was required in order to insure that any transmitted signal would be received, regardless of the orientation of the transmitting antenna or the atmospheric effects on the polarization of the transmitted signal.

An electric-magnetic dipole antenna was chosen for the antenna principally because of its broad beamwidth and because it is possible to obtain elliptical polarization at every (non-zero) point in space.

A theoretical discussion is given first, including the calculated radiation patterns. This is followed by a description of the construction techniques used in building the antenna. Finally, an evaluation of the experimentally obtained radiation patterns is given.

II. THEORETICAL DEVELOPMENT

Consider a right-handed Cartesian coordinate system which contains a loop antenna, with center at the origin lying in the X-Y plane, and a half-wave dipole antenna lying along the z axis. Figure 1 is a diagram of the antenna and its associated coordinate system.

An expression of the radiation field of the thin linear dipole may be found in the following manner.[1] Assuming a monochromatic sinusoidal current distribution along the antenna (refer to Figure 2), the retarded value of current at any point z along the antenna referred to any point in space at a distance s may be expressed as

$$\left[I\right] = I_o \sin\left[k\left(\frac{L}{2} \pm z\right)\right] e^{j(\omega t - ks)} \tag{1}$$

where $k = (2\pi/\lambda)$, and I_o is the maximum amplitude of the current.

Each element of length dz is considered to be an infinitesimal dipole whose contribution to the Fraunhofer field is given by

$$dH_\phi = j \frac{\sin\theta}{2\lambda s} \left[I\right] dz \tag{2}$$

The total field is given by the summation of all partial fields, and is

---

[1] John D. Kraus, Antennas (New York: McGraw Hill Book Company, Inc., 1950), p. 141.

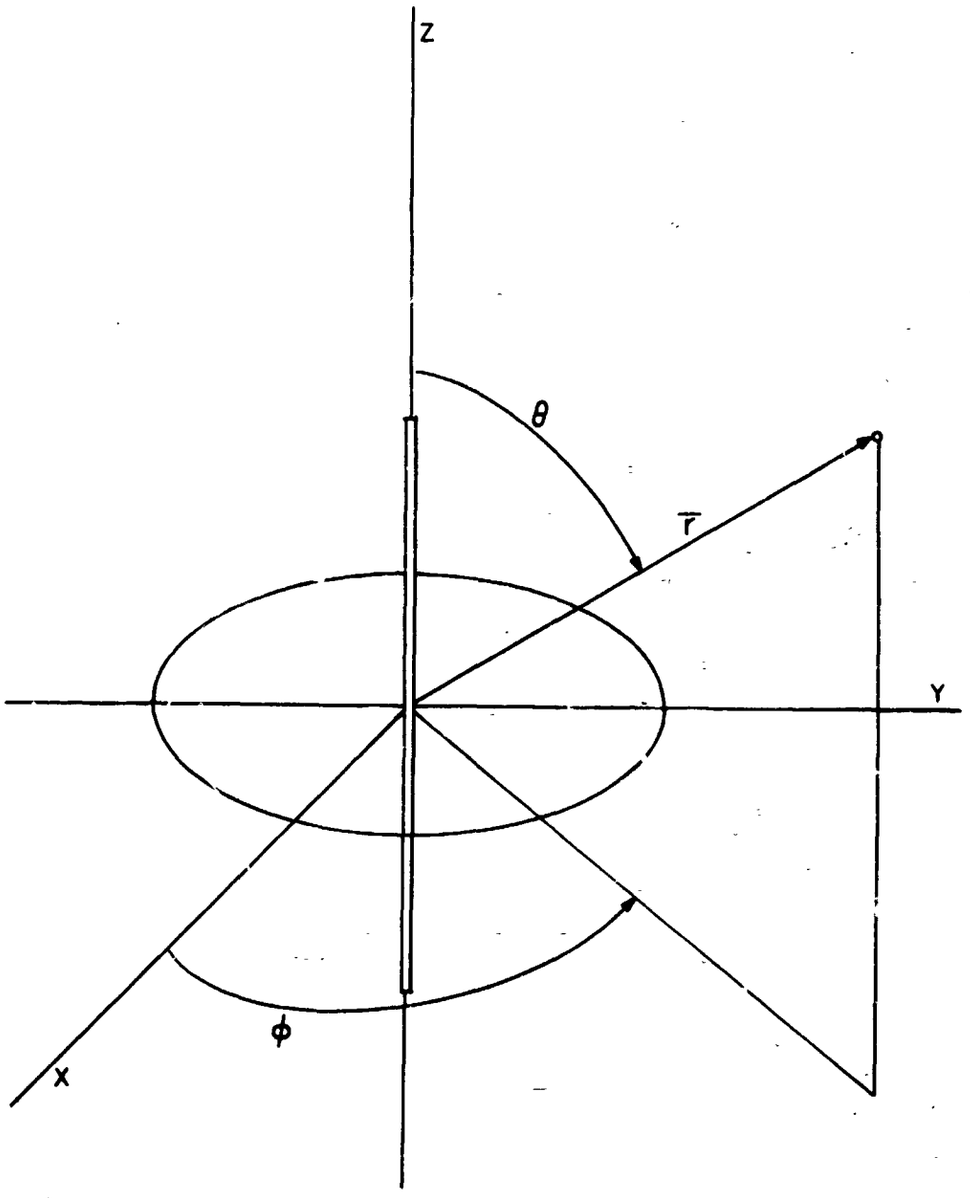

Fig. 1. - The Coordinate System Showing Antenna Orientation

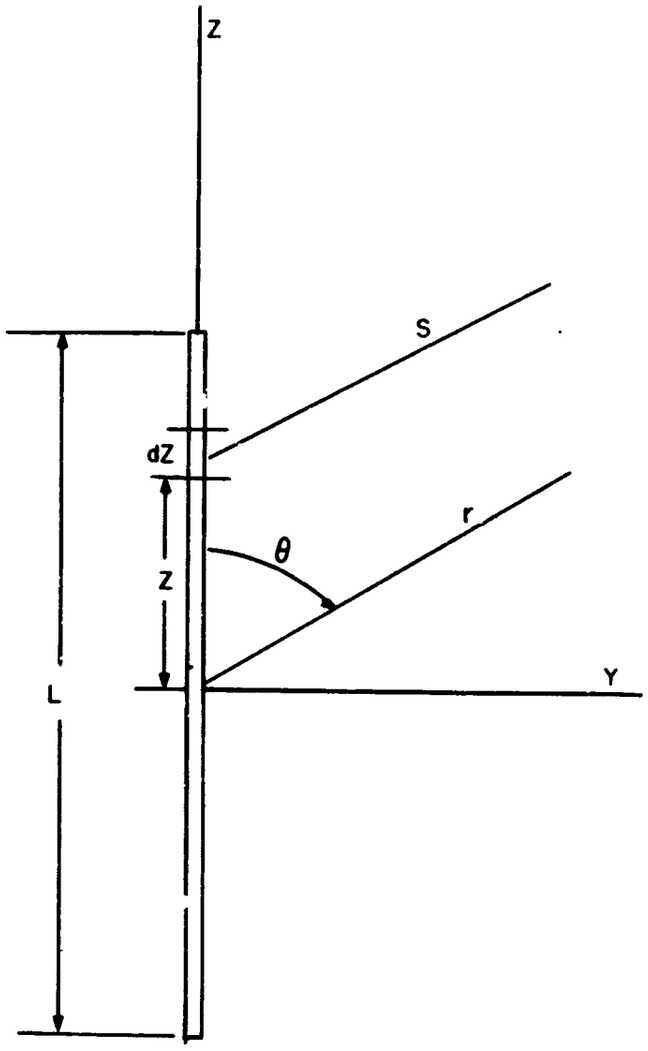

Fig. 2. - The Figure for the Derivation of the Field of a Thin-Linear Antenna

$$H_\phi = \int_{-(L/2)}^{L/2} dH_\phi \tag{3}$$

Substituting (1) and (2) into (3),

$$H_\phi = \int_{-(L/2)}^{L/2} j \frac{\sin\theta}{2\lambda s} I_o e^{j\omega t} e^{-jks} \sin\left[k\left(\frac{L}{2} \pm z\right)\right] dz \tag{4}$$

Expanding (4),

$$H = j \frac{I_o e^{j\omega t} \sin\theta}{2\lambda} \left[\int_{-(L/2)}^{o} \frac{e^{-jks}}{s} \sin\left(k\left(\frac{L}{2} + z\right)\right) dz \right. \tag{5}$$

$$\left. + \int_{o}^{L/2} \frac{e^{-jks}}{s} \sin\left(k\left(\frac{L}{2} - z\right)\right) dz \right]$$

The phase relationship between the distance s from any point on the antenna, and the distance r from the phase center of the antenna is

$$s = r - z \cos\theta \tag{6}$$

if $r \gg L$. The amplitude difference over the two paths is negligible at great distances.

Thus, (4) may be expressed as

$$H_\phi = \left[j \frac{I_o \sin\theta}{2\lambda} \frac{e^{j(\omega t - kr)}}{r} \right] \left[\int_{-(L/2)}^{o} e^{jkz\cos\theta} \sin\left(k \left(\frac{L}{2} + z \right) \right) dz \right. \tag{7}$$

$$\left. + \int_{o}^{L/2} e^{jkz\cos\theta} \sin\left(k \left(\frac{L}{2} - z \right) \right) dz \right]$$

These integrals are in the form

$$\int e^{ax} \sin(c+bx)dx = \frac{e^{ax}}{a^2 + b^2} \left[a\sin(c+bx) - b\cos(c+bx) \right] \tag{8}$$

Evaluation of the two integrals of (7) yields

$$\int_{-(L/2)}^{o} e^{jkz\cos\theta} \sin\left(k \left(\frac{L}{2} + z \right) \right) dz = \frac{1}{k\sin^2\theta} \tag{9}$$

$$\left[j\cos\theta \sin\frac{kL}{2} + \cos\frac{kL}{2} - e^{-jk(L/2)\cos\theta} \right]$$

and

$$\int_0^{L/2} e^{jkz\cos\theta} \sin\left(k\left(\frac{L}{2} - z\right)\right) dz = \frac{1}{k\sin^2\theta}$$

$$\left[-e^{jk(L/2)\cos\theta} - j\cos\theta\sin\frac{kL}{2} - \cos\frac{kL}{2}\right] \tag{10}$$

Substituting (9) and (10) into (7) and simplifying gives

$$H_\phi = \left[j\frac{I_o e^{j(\omega t - kr)}}{\lambda r}\right]\left[\frac{1}{k\sin\theta}\right]\left[\cos\left(k\frac{L}{2}\cos\theta\right) - \cos\left(k\frac{L}{2}\right)\right] \tag{11}$$

For a half-wavelength antenna, (11) reduces to

$$H_\phi = j\frac{I_o e^{j(\omega t - kr)}}{2\pi r}\frac{\cos\left(\frac{\pi}{2}\cos\theta\right)}{\sin\theta} \tag{12}$$

In the far field,

$$E_\theta = 120\pi H_\phi \tag{13}$$

so

$$E_\theta = j60I_o\frac{e^{j(\omega t - kr)}}{r}\frac{\cos\left(\frac{\pi}{2}\cos\theta\right)}{\sin\theta} \tag{14}$$

Figure A-1 shows the field pattern of E_θ as a function of the coordinate θ. Note that (14) has no dependence on the coordinate ϕ; that is, in the ϕ plane the radiation pattern is a circle.

The expression for the radiation field of the loop may be derived using the concept of the vector potential, $\bar{A}$, in the following manner. Figure 3 is a diagram of a loop lying in the XY plane and supporting a uniform current I_o, which has a time dependence given by

$$i(t) = \mathrm{Re} I_o e^{j\omega t} \tag{15}$$

The vector potential at any point in space is given by

$$\bar{A} = \frac{\mu}{4\pi} \int_v \bar{J}\,(\bar{r}\,) \frac{e^{-jkR}}{R}\, dv' \tag{16}$$

In the case of the plane loop, (16) reduces to

$$\bar{A} = \frac{\mu}{4\pi} \int_0^{2\pi} I_o e^{j\omega t} a \frac{e^{-jkR}}{R}\, \bar{a}_{\phi'}\, d\phi' \tag{17}$$

From Figure 3 it can be shown that

$$\cos\zeta = \sin\theta\cos\left[\phi' - \phi\right] \tag{18}$$

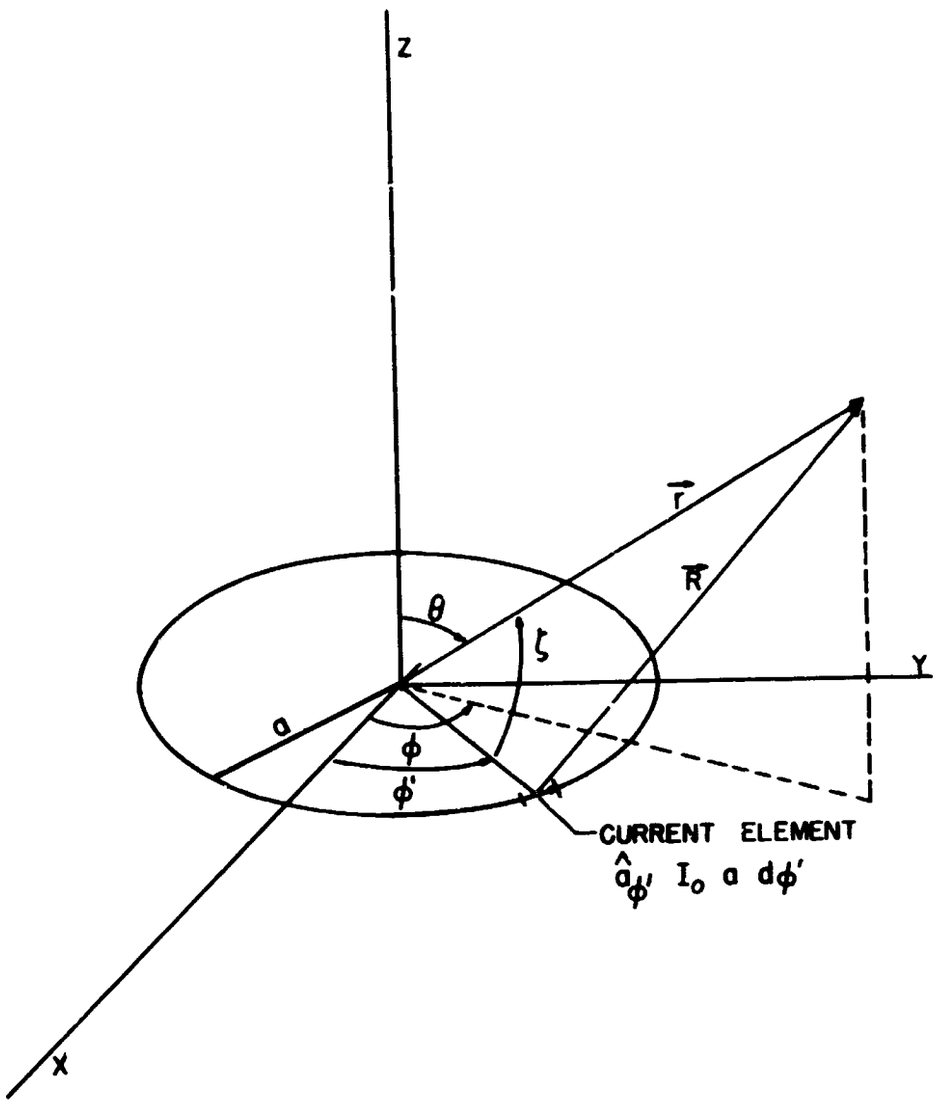

Fig. 3. - The Figure for the Derivation of the Field of a Loop Antenna.

Also, at a point in the far-field of the antenna it can be shown that an approximate expression for R is

$$R = r - a\cos\psi \tag{19}$$

and an approximate expression for (1/R) is

$$(1/R) = (1/r) \tag{20}$$

under the assumption that $R \gg a$.

Equation (17) may now be written as

$$\bar{A} = \frac{\mu I_o e^{j(\omega t - kr)} a}{4\pi r} \int_o^{2\pi} \bar{a}_{\phi'} e^{jka\cos(\phi'-\phi)\sin\theta} \, d(\phi'-\phi) \tag{21}$$

Making the following two substitutions

$$\gamma = \phi' - \phi \tag{22}$$

$$\bar{a}_{\phi'} = -\bar{a}_x \sin\phi' + \bar{a}_y \cos\phi' \tag{23}$$

(21) becomes

$$\bar{A} = \frac{\mu I_o a e^{j(\omega t - kr)}}{4\pi r} \int_{-\phi}^{2\pi-\phi} \left[-\bar{a}_x \sin(\gamma + \phi) + \bar{a}_y \cos(\gamma + \phi) \right] \times \left(e^{jka\cos\gamma\sin\theta} d\gamma \right) . \tag{24}$$

Expanding (24) and collecting terms,

$$\bar{A} = \frac{\mu I_o a e^{j(\omega t - kr)}}{4\pi r} \left(\int_{-\phi}^{2\pi-\phi} (-\bar{a}_x \sin\phi + \bar{a}_y \cos\phi) \cos\gamma e^{jka\cos\gamma\sin\theta} d\gamma \right. \tag{25}$$

$$\left. + \int_{-\phi}^{2\pi-\phi} (-\bar{a}_x \cos\phi - \bar{a}_y \sin\phi) \sin\gamma e^{jka\cos\gamma\sin\theta} d\gamma \right)$$

Substituting the following two expressions

$$\bar{a}_\phi = \bar{a}_x \sin\phi + \bar{a}_y \cos\phi \tag{26}$$

$$\bar{a}_n = \bar{a}_x \cos\phi + \bar{a}_y \sin\phi \tag{27}$$

into (25) yields

$$\bar{A} = \frac{\mu I_o a e^{j(\omega t - kr)}}{4\pi r} \left[\bar{a}_\phi \int_{-\phi}^{2\pi-\phi} \cos\gamma e^{jka\cos\gamma\sin\theta} \, d\gamma \right.$$

$$\left. - \bar{a}_n \int_{-\phi}^{2\pi-\phi} \sin\gamma e^{jka\cos\gamma\sin\theta} \, d\gamma \right] \tag{28}$$

The second integral is equal to zero. The first integral is evaluated in the following manner

$$\int_{-\phi}^{2\pi-\phi} \cos\gamma e^{jka\cos\gamma\sin\theta} \, d\gamma = \int_{-\phi}^{2\pi-\phi} \left[\sum_{n=0}^{\infty} \frac{(jka\cos\gamma\sin\theta)^n}{n!} \right] \cos\gamma d\gamma \tag{29}$$

$$= \sum_{n=0}^{\infty} \left[\frac{(jka\sin\theta)^n}{n!} \int_{-\phi}^{2\pi-\phi} (\cos\gamma)^{n+1} \, d\gamma \right] \tag{30}$$

The binomial expansion of the integrand is

$$(\cos\gamma)^{n+1} = \frac{1}{2^{n+1}} \sum_{s=0}^{n+1} \frac{(n+1)!}{s!(n+1-s)!} e^{j(n+1-2s)\gamma} \tag{31}$$

Thus,

$$\int_{-\phi}^{2\pi-\phi} (\cos\gamma)^{n+1}\, d\gamma = \frac{(n+1)!}{\left[\left(\frac{n+1}{2}\right)!\right]^2} \quad \frac{2\pi}{2^{n+1}} \tag{32}$$

for n odd. When n is even, the integral is zero.

Substituting (32) into (30)

$$\int_{-\phi}^{2\pi-\phi} \cos\gamma e^{jka\cos\gamma\sin\theta} = \sum_{n\ \text{odd}}^{\infty} \frac{(jka\sin\theta)^n}{n!} \quad \frac{(n+1)!}{\left[\left(\frac{n+1}{2}\right)!\right]^2} \quad \frac{2\pi}{2^{n+1}} \tag{33}$$

or

$$\int_{-\phi}^{2\pi-\phi} \cos\gamma e^{jka\cos\gamma\sin\theta} = 2\pi j \sum_{n=0}^{\infty} (-1)^n \quad \frac{\left(\frac{ka\sin\theta}{2}\right)^{1+2n}}{n!(n+1)!} \tag{34}$$

The series representation of an p-th order Bessel function of the first kind is given by

$$J_p(x) = \sum_{n=0}^{\infty} \frac{(-1)^p\ (x/2)^{p+2n}}{p!\ (n+p)!} \tag{35}$$

Equation (28) is then simplified to

$$\bar{A}_\phi = \frac{\mu I_o a e^{j(\omega t - kr)}}{4\pi r} \left[\bar{a}_\phi 2\pi j J_1(ka\sin\theta) \right] \tag{36}$$

Simplifying (36) yields

$$\bar{A} = j \frac{\mu I_o a e^{j(\omega t - kr)}}{2r} J_1(ka\sin\theta)\, \bar{a}_\phi \tag{37}$$

Equation (37) expresses the vector potential at any coordinate point in the far field of the loop. In the far field the electric field intensity is related to the vector potential by

$$\bar{E} = - j\omega\bar{A} \tag{38}$$

Finally, then,

$$E_\phi = - \frac{\omega\mu}{2} I_o a \frac{e^{j(\omega t - kr)}}{r} J_1(ka\sin\theta) \tag{39}$$

For $a = (\pi/8)\lambda$, (39) becomes

$$E_\phi = \frac{- \pi\eta I_o a e^{j(\omega t - kr)}}{2\lambda r} J_1 \left(\frac{\pi}{4} \sin\theta \right) \tag{40}$$

where $\eta = 120\pi$. Also,

$$H_\Theta = \frac{-\pi I_o a e^{j(\omega t - kr)}}{2\lambda r} J_1 \left(\frac{\pi}{4} \sin\Theta \right) \qquad (41)$$

Figure A-2 shows the field pattern of E_ϕ as a function of the coordinate Θ. Note that (40) has no dependence on the coordinate ϕ.

A comparison of the field expressions (12) and (39) and the radiation patterns of the dipole and the loop shows that there is a fundamental phase quadrature between the fields of the two. This was pointed out by Kandoian in 1946.[2] The radiation patterns of a horizontal loop with a circumference less than six-tenths of a wavelength[3] and a dipole perpendicular to the loop are essentially the same. "Thus," says Kandoian, "at every point in space equal amounts of horizontal and vertical polarization will be obtained, if the available power is equally divided."

Proper phasing of the two elements will yield any desired polarization. Circular polarization is obtained if the currents on the loop and dipole are in phase and if the amplitudes of the radiated fields are equal.

---

[2]A. G. Kandoian, "Three New Antenna Types and Their Application," Proceedings of the IRE, 34:70W-77W, February, 1946.

[3]Donald G. Foster, "Loop Antennas With Uniform Current," Proceedings of the IRE, 32:603-607, October, 1944.

III. DESIGN AND CONSTRUCTION OF THE ANTENNA

A photograph of the antenna is shown in Figure 4. The inner hub consists of two pieces of two and one-half inch diameter Rexolite, each of which holds a section of the electric dipole, secured by a setscrew. Three-quarter inch Rexolite rods extend radially from the hub to support the loop. The hub is tapped and the rods are threaded and screwed into the hub.

The dipole sections are half-inch diameter aluminum rods, tapered at the end from which they are fed to provide a smooth impedance transformation. Quarter-inch brass screws are inserted into the rods to permit the feed line to be soldered to the dipole section.

The loop is made of quarter-inch copper tubing. Its radius is approximately one-quarter of a wavelength, or twenty-one inches.

Half-wave coaxial cable baluns at the feed point of the dipole and loop provide balance for the system with respect to ground. The balun also acts as an impedance transformer, causing the impedance seen looking into the terminals of the balun to be one-fourth as great as the antenna impedance without the balun.

The input impedance of a half-wave center-fed thin linear antenna is approximately 73 + j43 ohms. The actual antenna length is about five per-cent shorter than one-half wavelength to reduce the reactive component. It also reduces the real component slightly.[4]

[4]Kraus, op. cit., p. 146.

Fig. 4. - A Photograph of the Electric-Magnetic Dipole Antenna

The input impedance of a loop antenna as a function of its length is presented in a report entitled "Loop Antenna Measurements".[5] Figure 18 of this report shows that a half-wavelength loop is at a resonant point, and any slight variation of length causes an extremely rapid change in reactance, so some compromise must be made in choosing its length. It was decided to use a diameter of one-quarter wavelength, or a circumferance of 0.785λ. The input impedance at this length is approximately 100 + j100.

Single-stub tuning is used to match the input impedances to the fifty-ohm feeder cable.

The input impedance measurements were made with the antenna in an anechoic chamber. Figure 5 shows a block diagram of the impedance measuring system. This system employs an admittance meter and a thirty-megacycle amplifier used as a null detector. The impedance of each element was measured and matched to fifty ohms with a single shorted stub.

---

[5]Phyllis A. Kennedy, "Loop Antenna Measurements," Technical Report Number 213, Figure 18, Cruft Laboratory, Harvard University, Cambridge, Massachusetts, 1955.

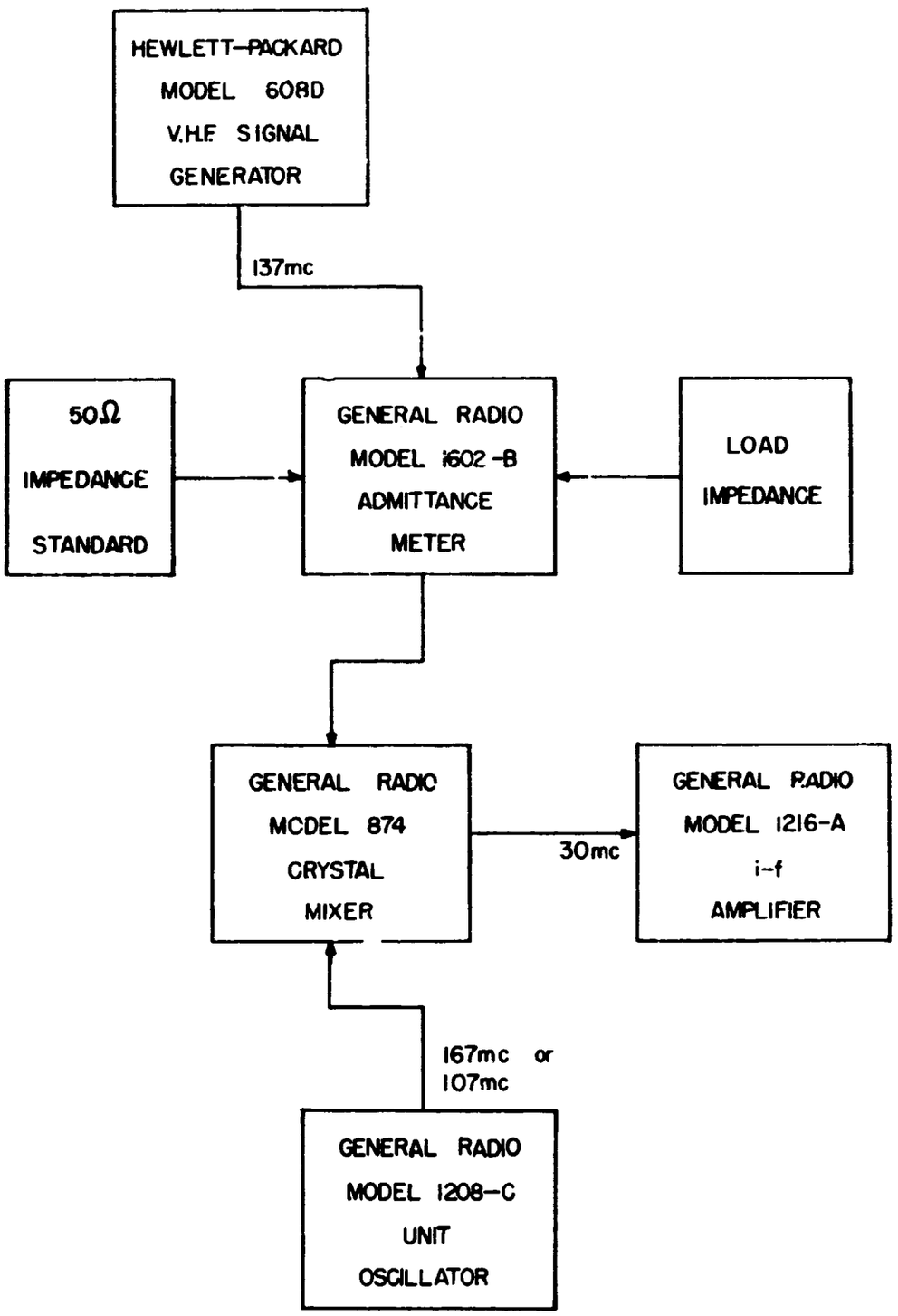

Fig. 5. - A Block Diagram of the Impedance Measuring System

IV. EVALUATION OF ANTENNA PERFORMANCE

The power patterns of the antenna were measured at an outdoor antenna range. By experimentally varying the phasing of the two elements and the amplitudes of the input signals, it was possible to obtain a signal that was within two decibels of being circularly polarized.

An azimuth pattern of the dipole element is shown in Figure B-1. This pattern was taken with the transmitting antenna vertically polarized, and the pattern corresponds very well to the theoretical pattern in Figure A-3.

The azimuth pattern of the loop element is shown in Figure B-2. It does not correspond as well to its theoretical pattern, (A-3), being slightly asymmetric. Since the loop is fairly large in electrical length, the current distribution is not uniform. The dip in the pattern was probably caused by the non-uniform current distribution and the feed line to the loop.

Figures B-3 and B-4 show polarization patterns of the complete antenna. B-3 was taken receiving a vertically polarized signal, and B-4 was taken receiving a horizontally polarized signal. These patterns illustrate that the degree of polarization is circular within two decibels.

Figures B-5 through B-11 show conical cuts of the antenna respectively at $\theta = 90^{\circ}$, 85°, 80°, 75°, 70°, 65°, and 60°. Model tower geometry restricted further cuts. These patterns indicate

the omnidirectional characteristics of the antenna. These patterns also indicate elliptical polarization of the received signal.

BIBLIOGRAPHY

Abramowitz, Milton and Irene A. Stegun. (eds.). Handbook of Mathematical Functions With Formulas, Graphs, and Mathematical Tables. National Bureau of Standards, United States Department of Commerce. Washington: Government Printing Office, 1964.

Foster, Donald. "Loop Antennas with Uniform Current," Proceedings of the I.R.E., 32:603-607, October, 1944.

Jasik, Henry. Antenna Engineering Handbook. New York: McGraw Hill Book Company, Inc., 1961.

Kandoian, A. G. "Three New Antenna Types and Their Applications," Proceedings of the I.R.E., 34:70W-77W, February, 1946.

Kennedy, Phyllis A. Loop Antenna Measurements. Technical Report Number 213, Cruft Laboratory, Harvard University, Cambridge, Massachusetts, 1955.

Kraus, John D. Antennas. New York: McGraw Hill Book Company, Inc. 1950.

Sichak, W. and S. Milazzo. "Antennas for Circular Polarization," Proceedings of the I.R.E., 36:999-1000, August, 1948.

Storer, James E. "The Impedance of Thin Wire Loop Antennas," AIEE Transactions, 75:606-18, November, 1956.

APPENDIX A

THE THEORETICAL RADIATION PATTERNS OF THE ANTENNA

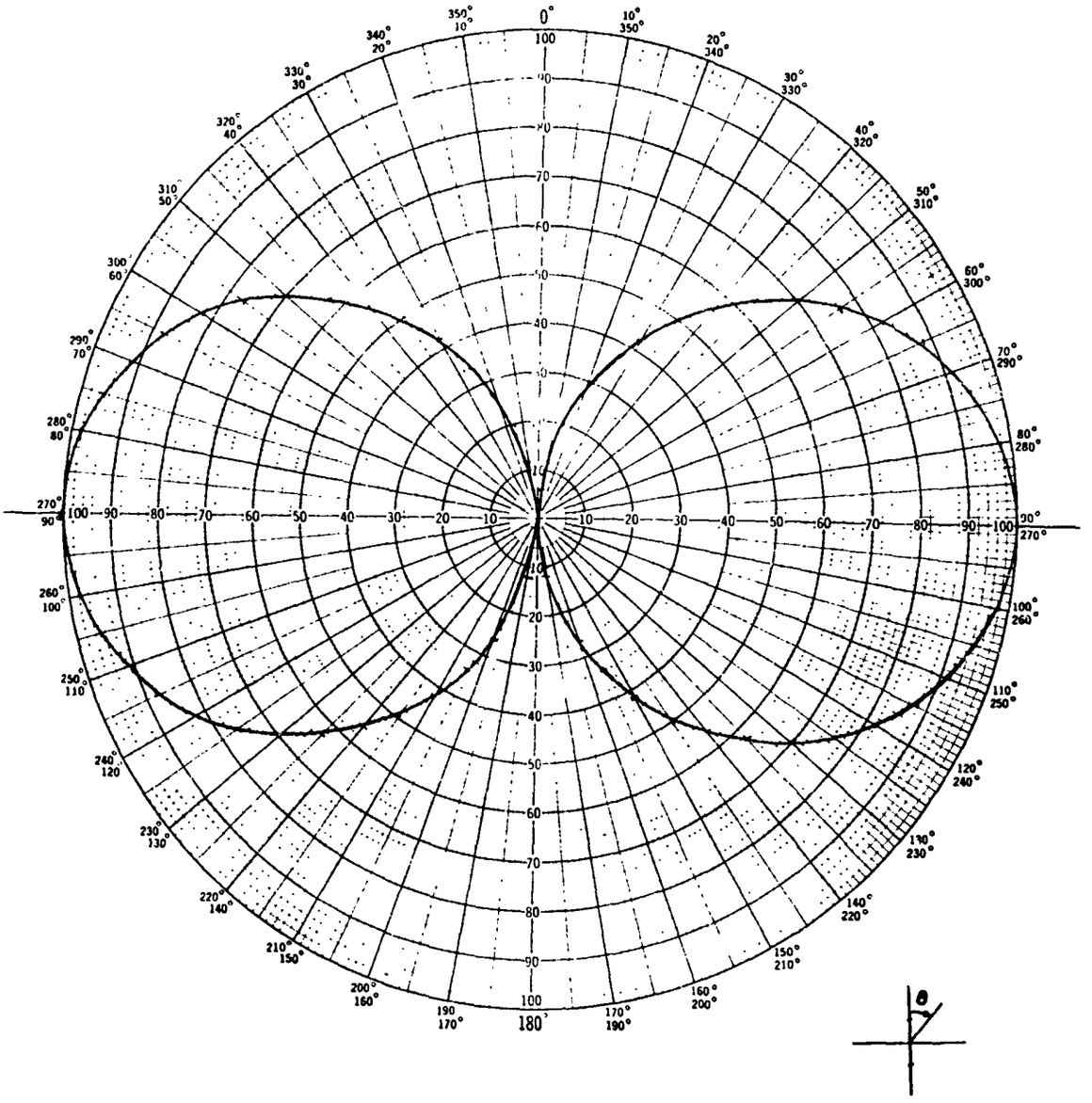

Fig. A-1. - The Radiation Field ot a Half-Wave Center-Fed Thin Linear Dipole

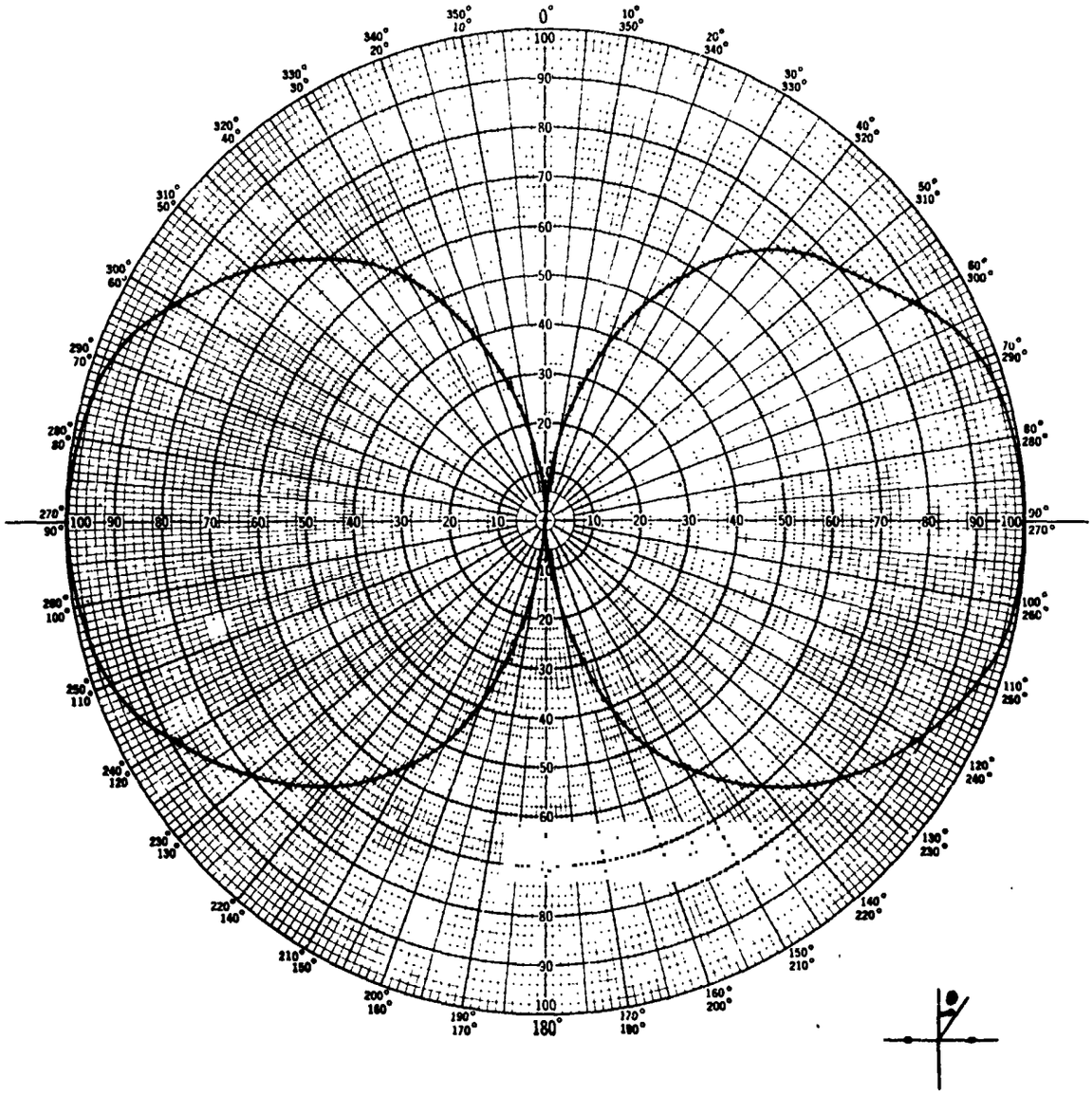

Fig. A-2. - The Radiation Field of a Loop Antenna With Uniform Current Distribution

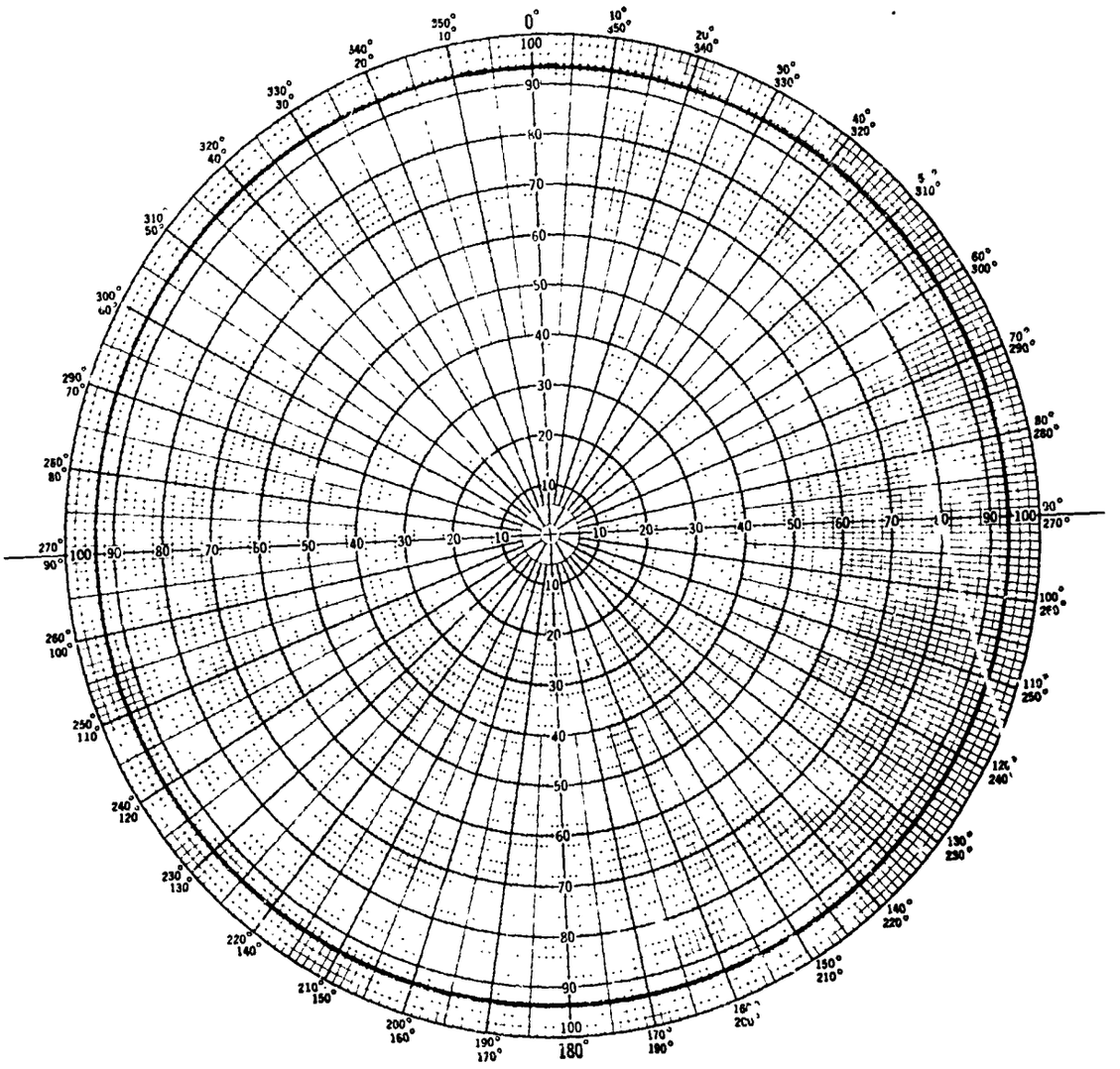

Fig. A-3. - The Theoretical Azimuth Pattern of a Loop or a Dipole

APPENDIX B

THE EXPERIMENTAL RADIATION PATTERNS OF THE ANTENNA

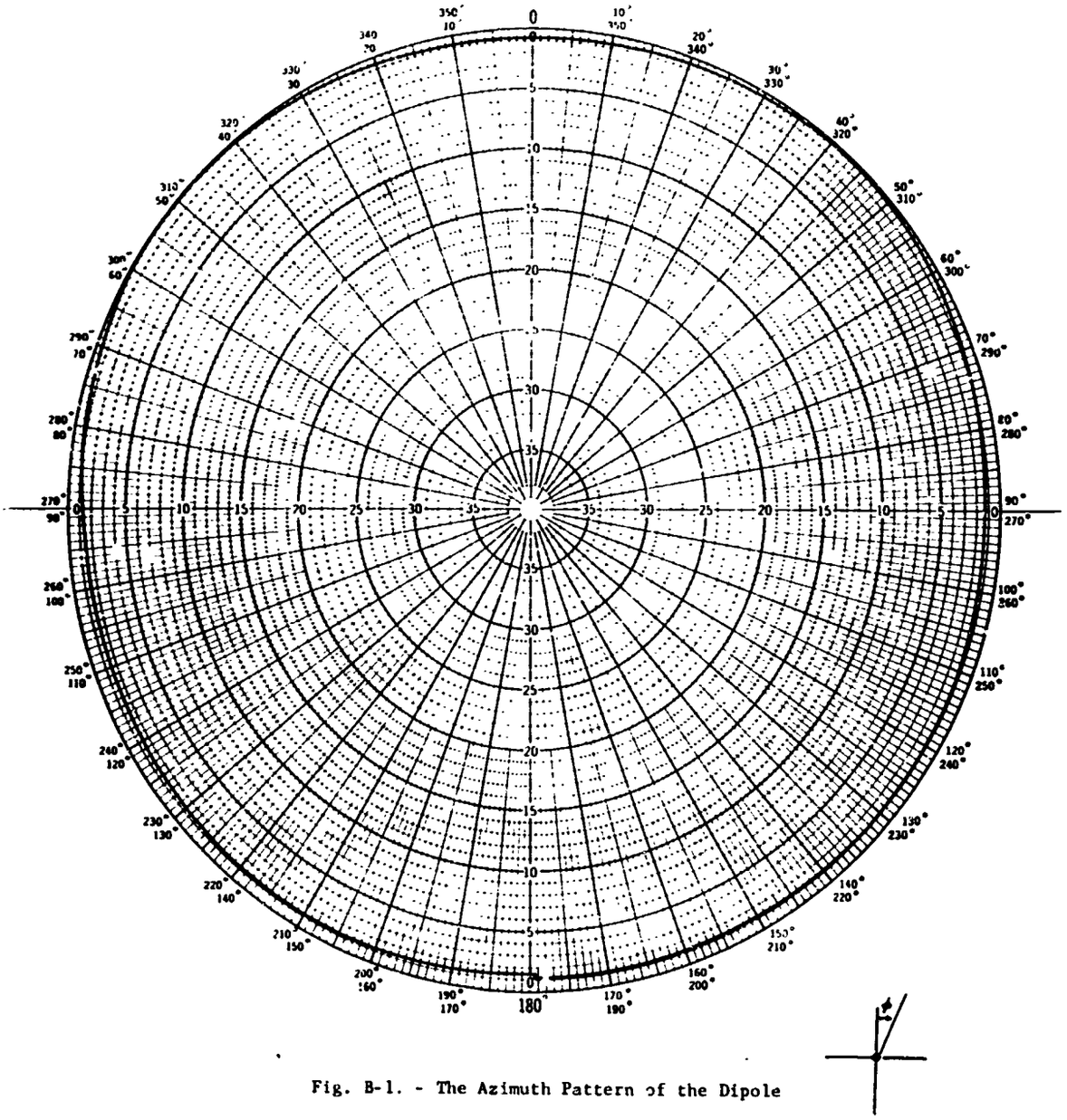

Fig. B-1. - The Azimuth Pattern of the Dipole

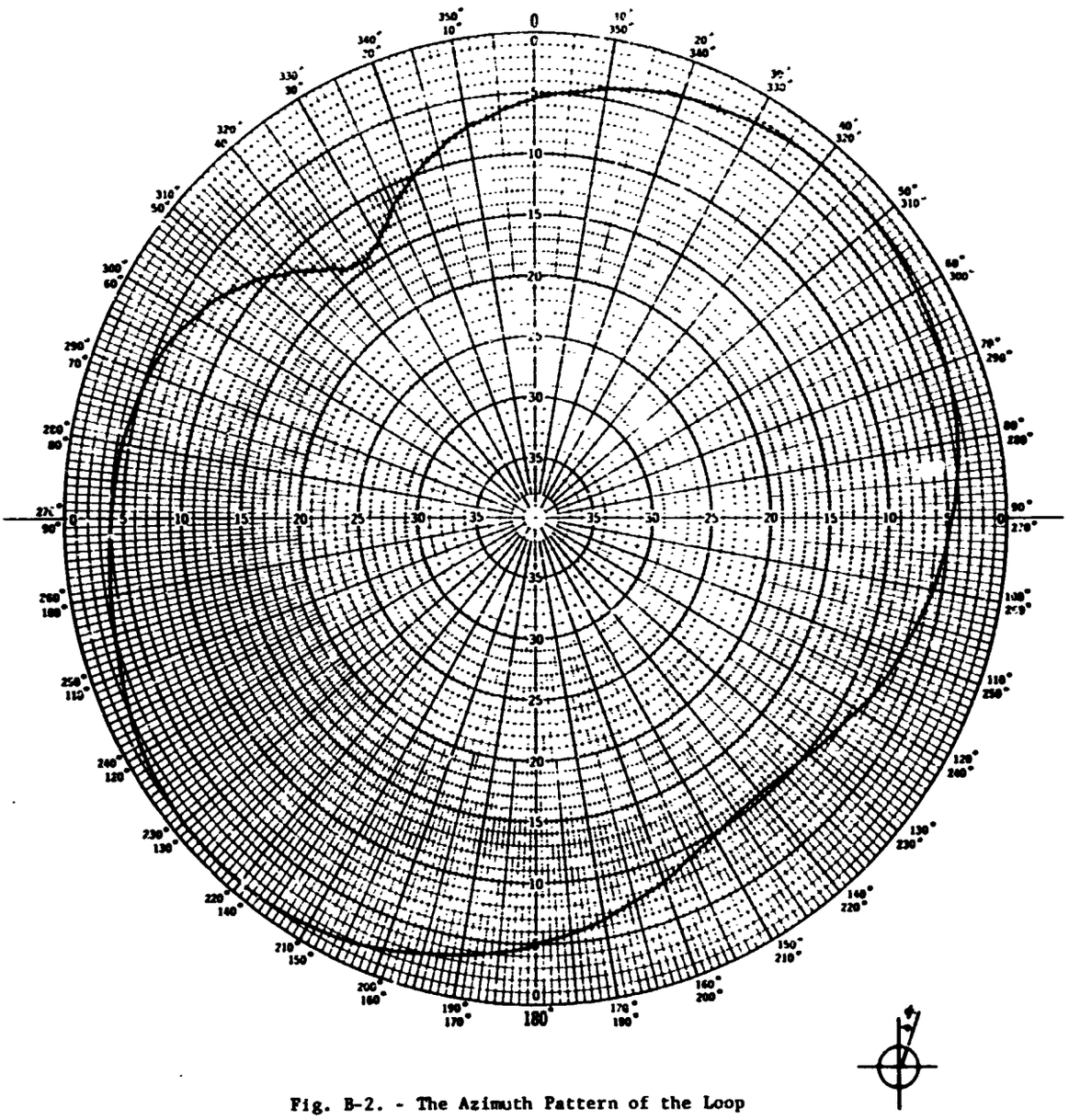

Fig. B-2. - The Azimuth Pattern of the Loop

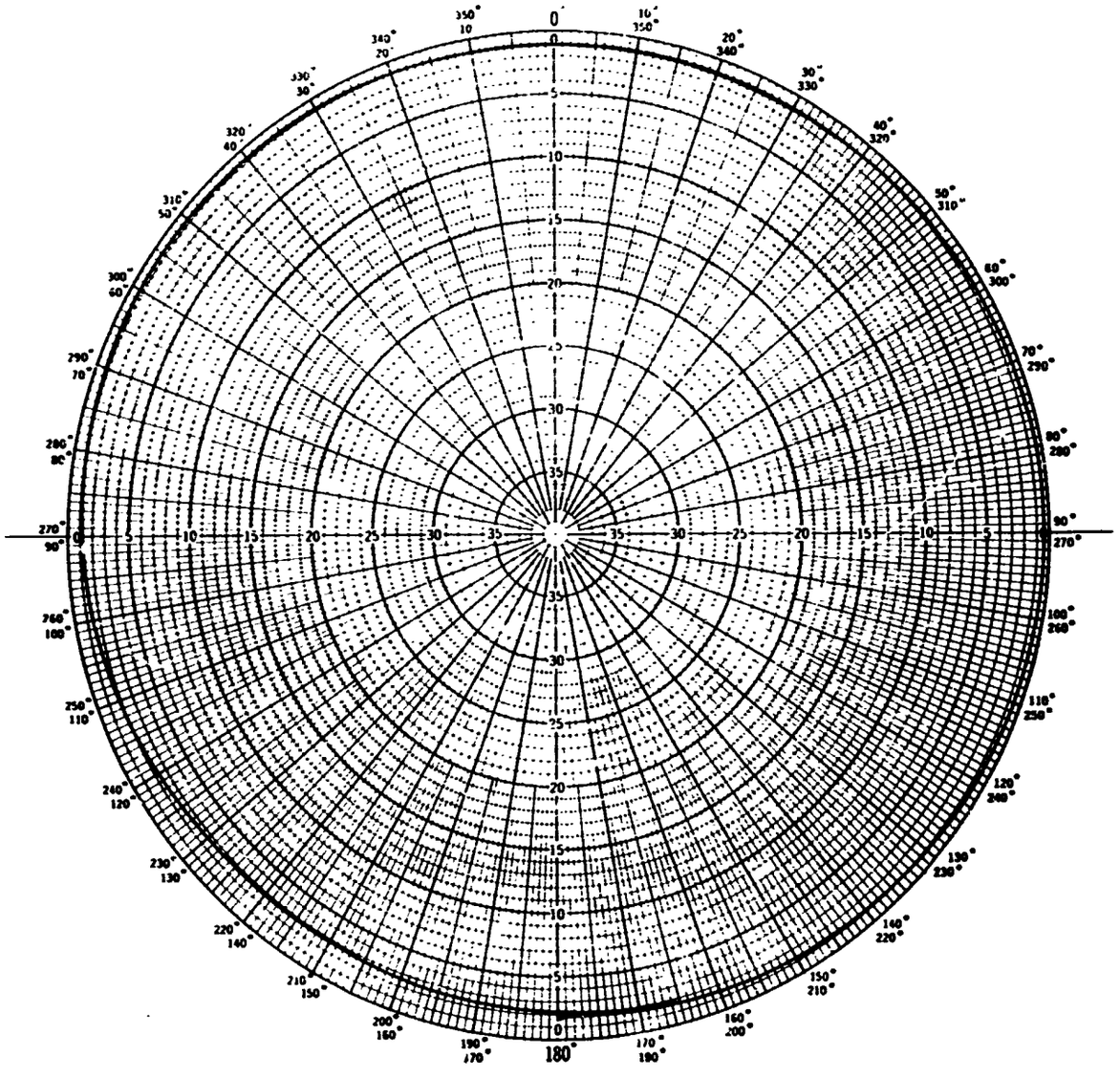

Fig. B-3. - The Polarization Pattern of the Antenna, Vertically Polarized Signal

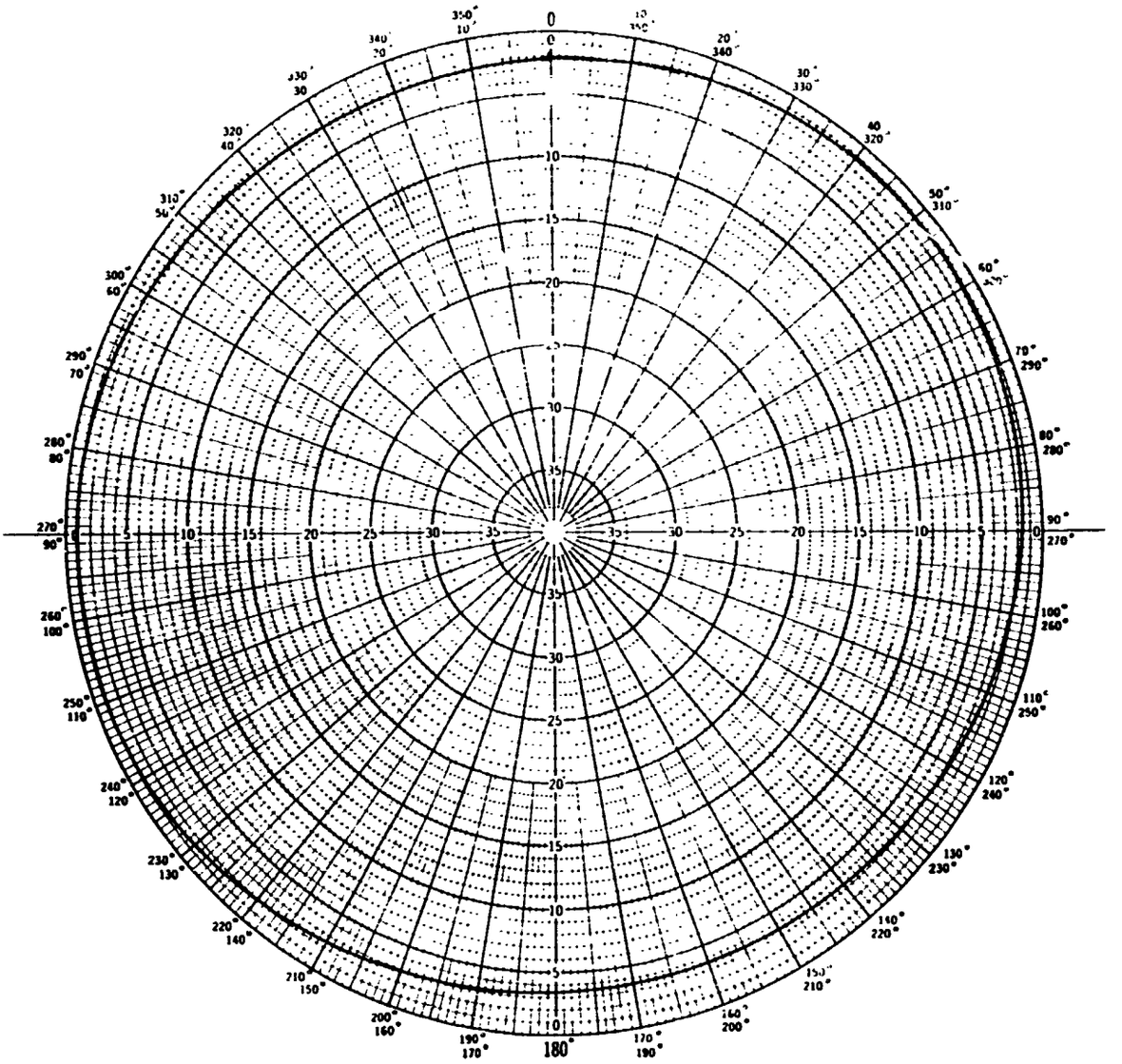

Fig. B-4. - The Polarization Pattern of Antenna, Horizontally Polarized Signal

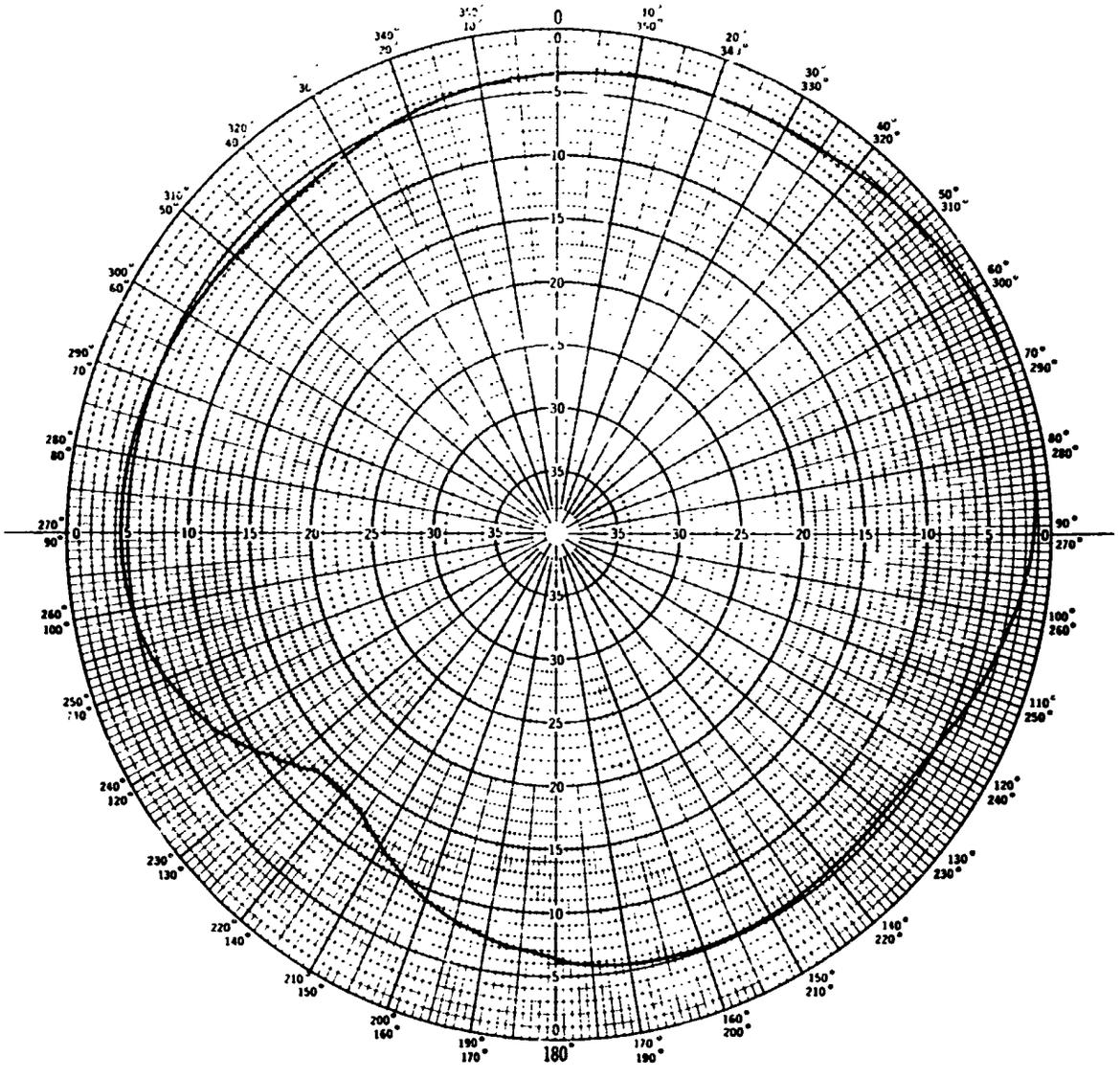

Fig. B-5. - A Conical Cut of the Antenna, $\theta = 90^{o}$

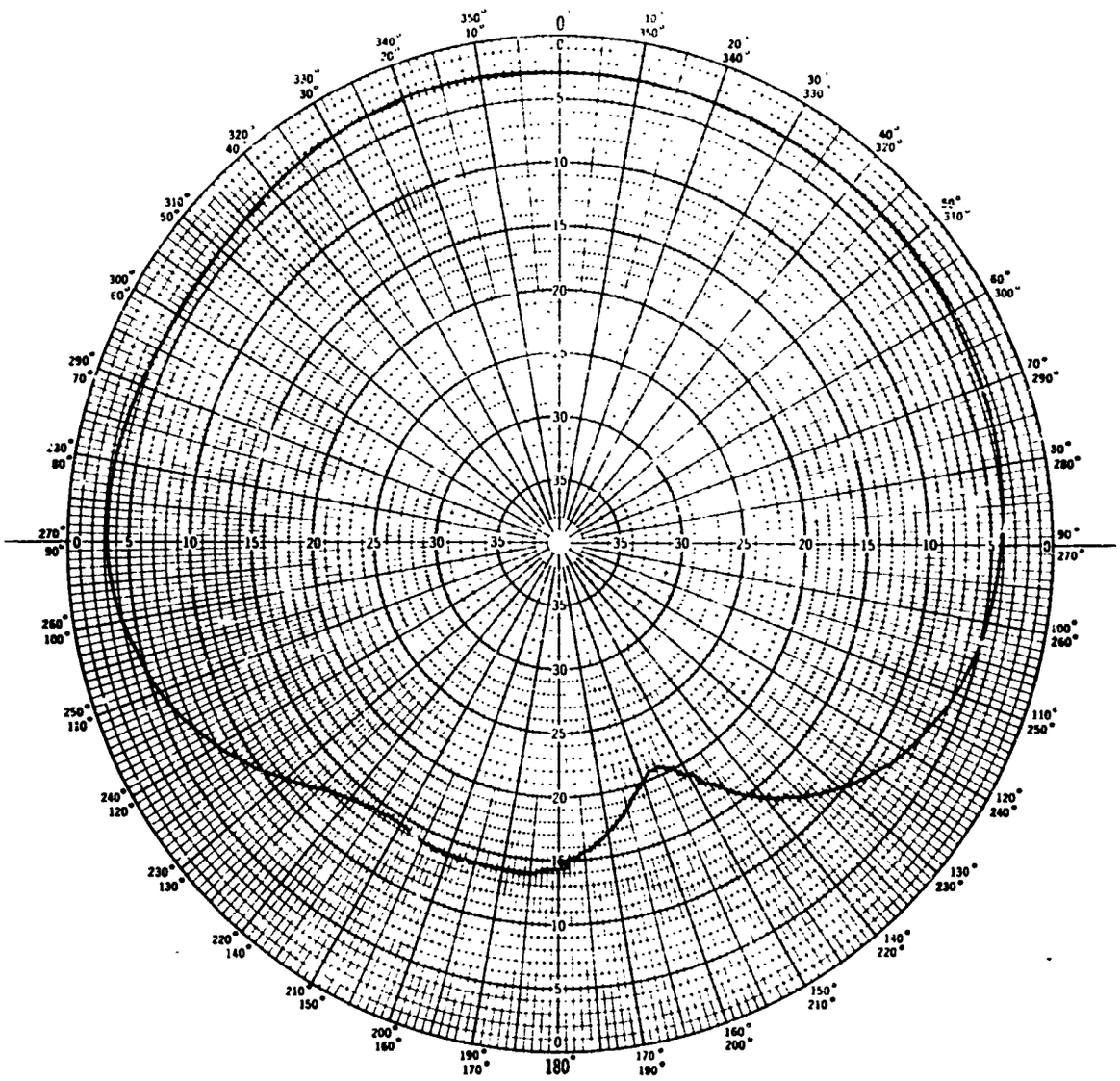

Fig. B-6. - A Conical Cut of the Antenna, $\theta = 85^{o}$

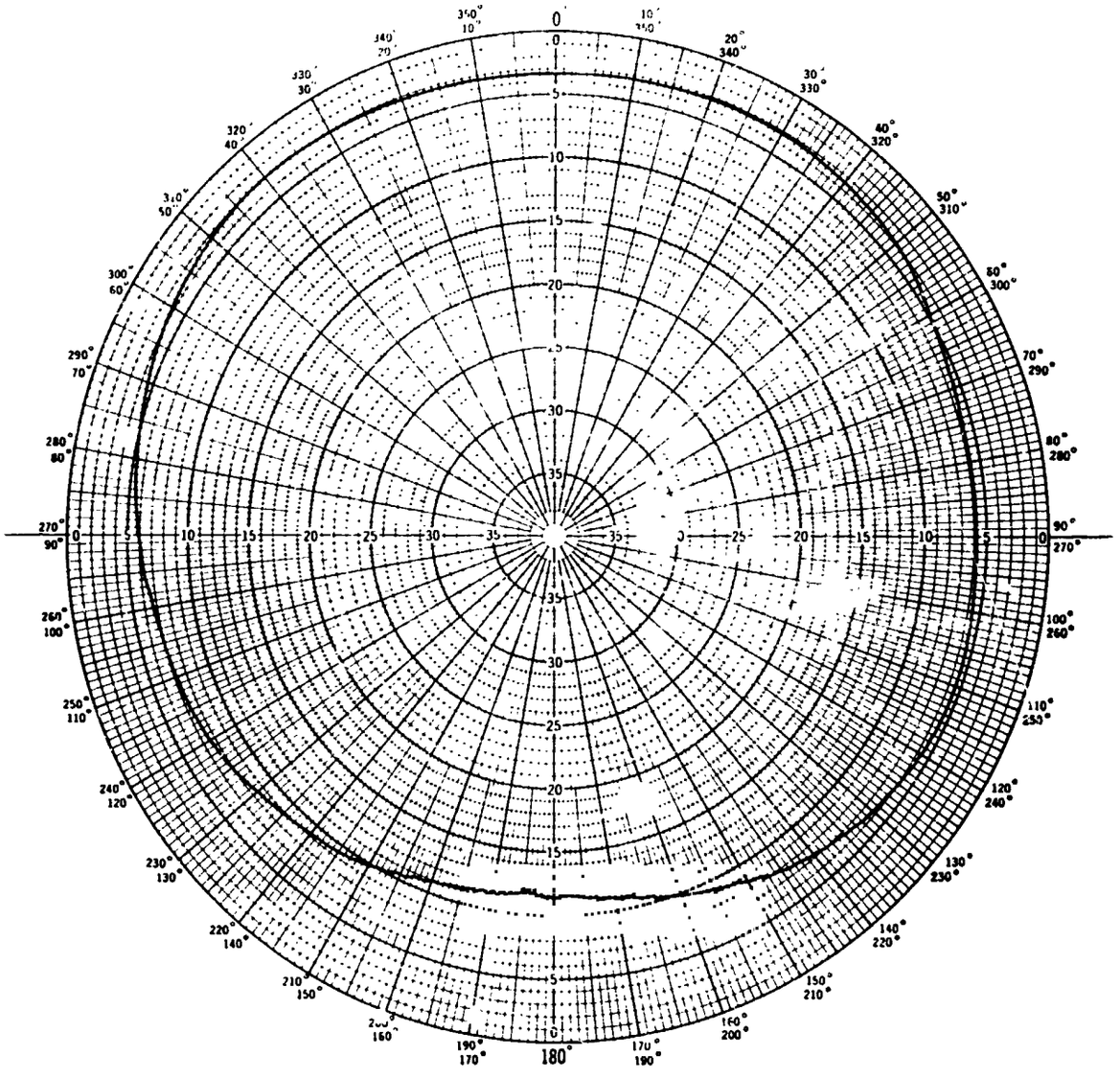

Fig. B-7. - A Conical Cut of the Antenna, $\theta = 80^{o}$

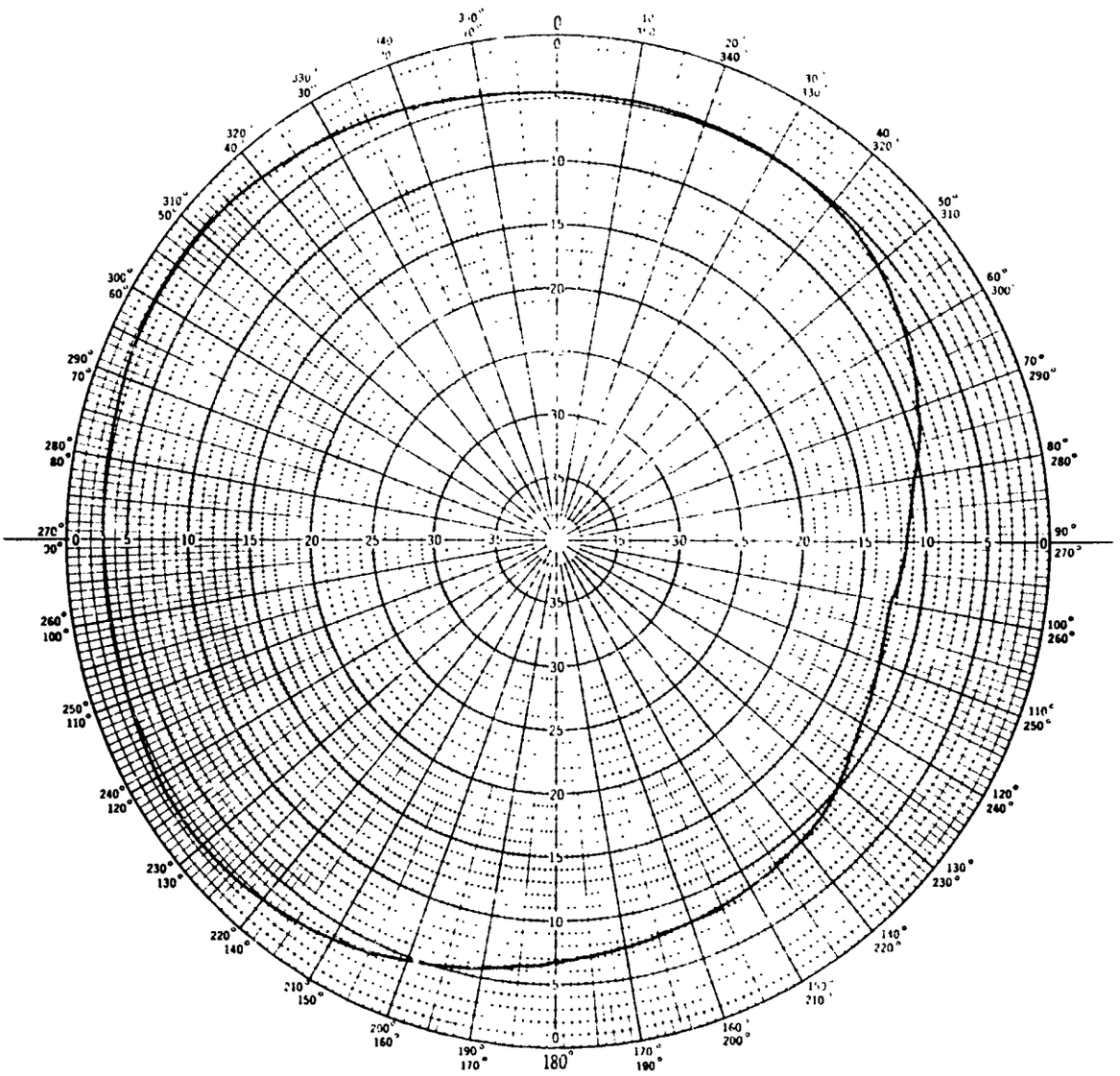

Fig. B-8. - A Conical Cut of the Antenna, $\Theta = 75^{\circ}$

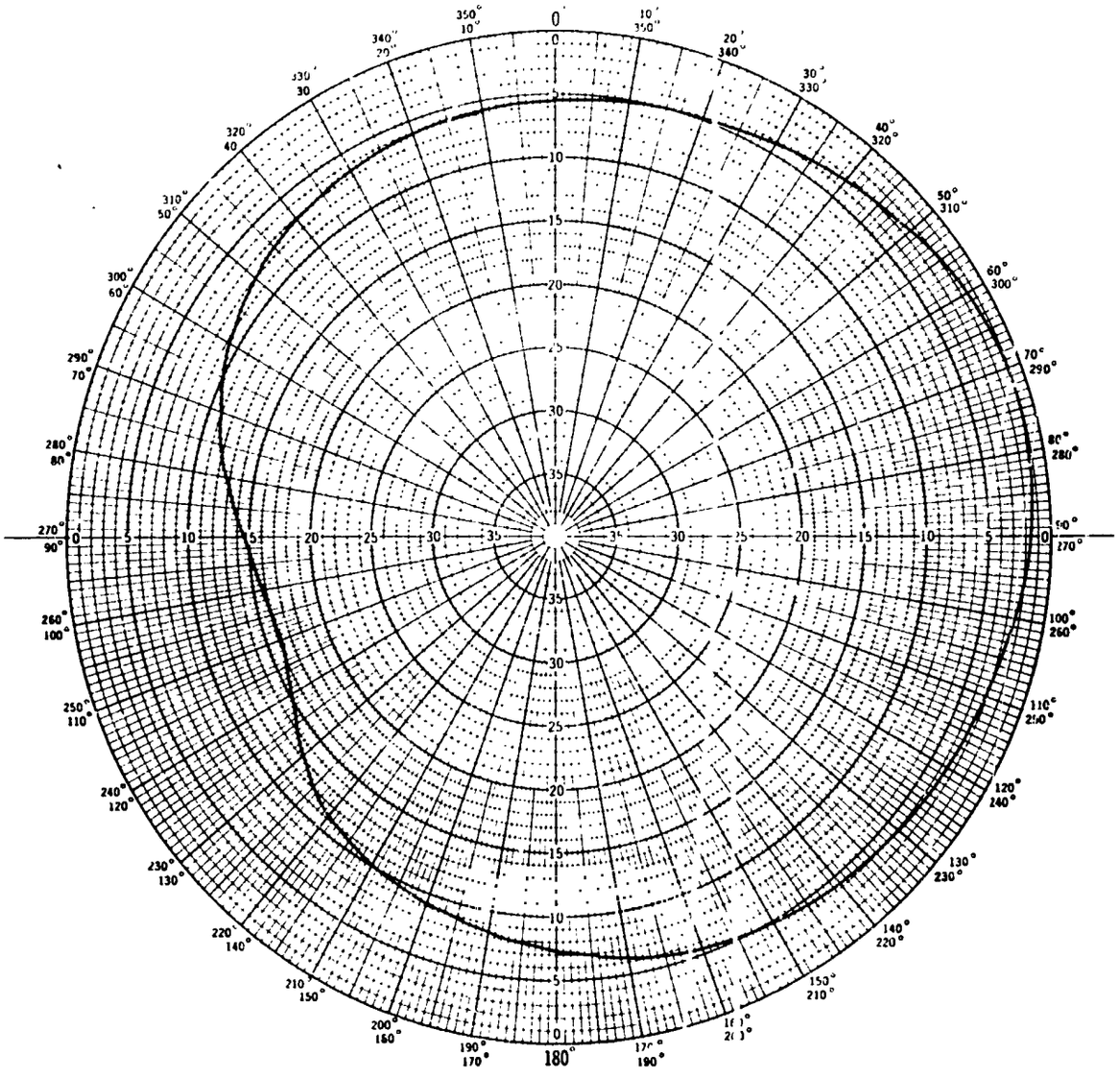

Fig. B-9. - A Conical Cut of the Antenna. $\theta = 70^{\circ}$

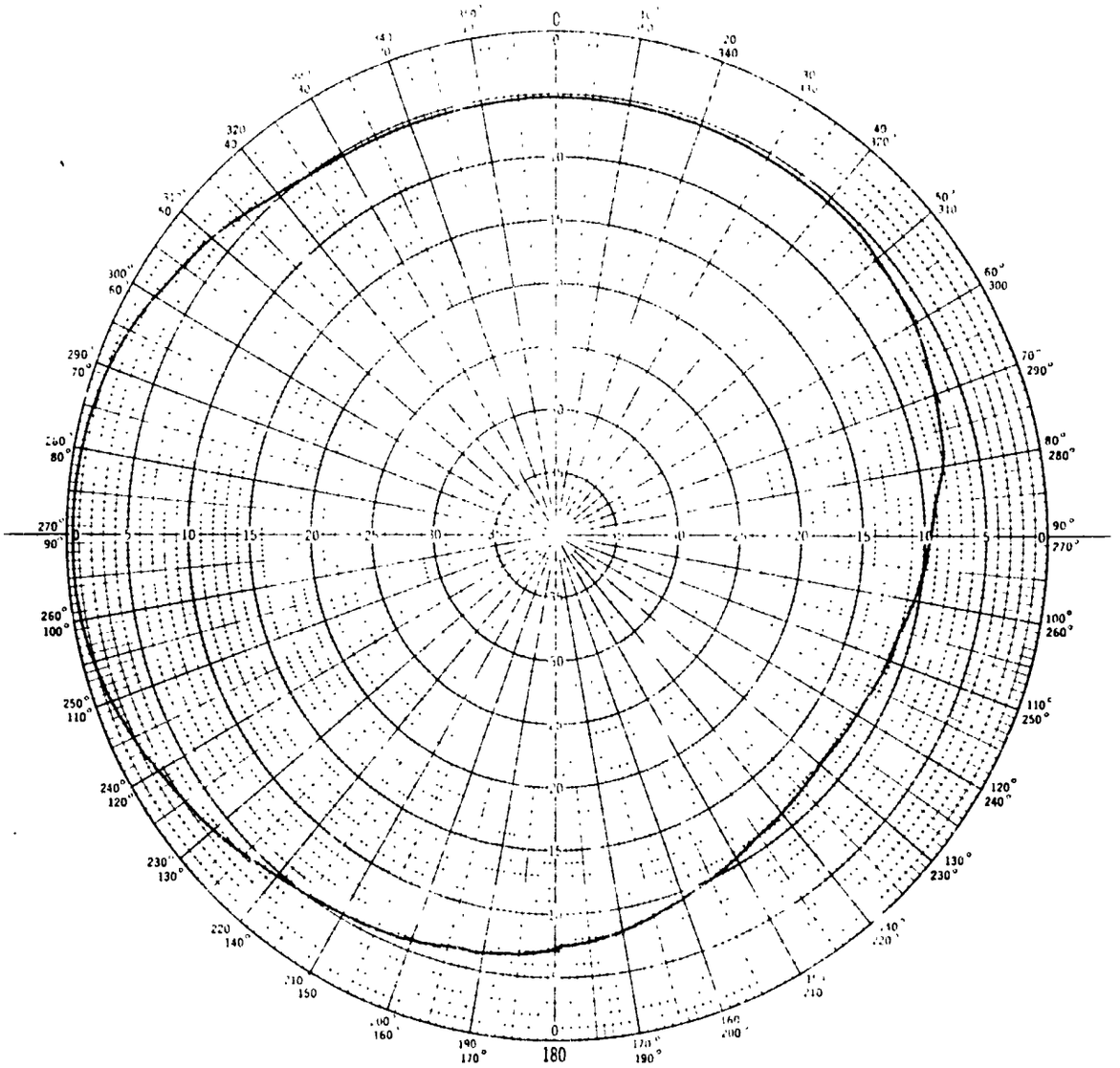

Fig. B-10. - A Conical Cut of the Antenna, $\theta = 65^{\circ}$

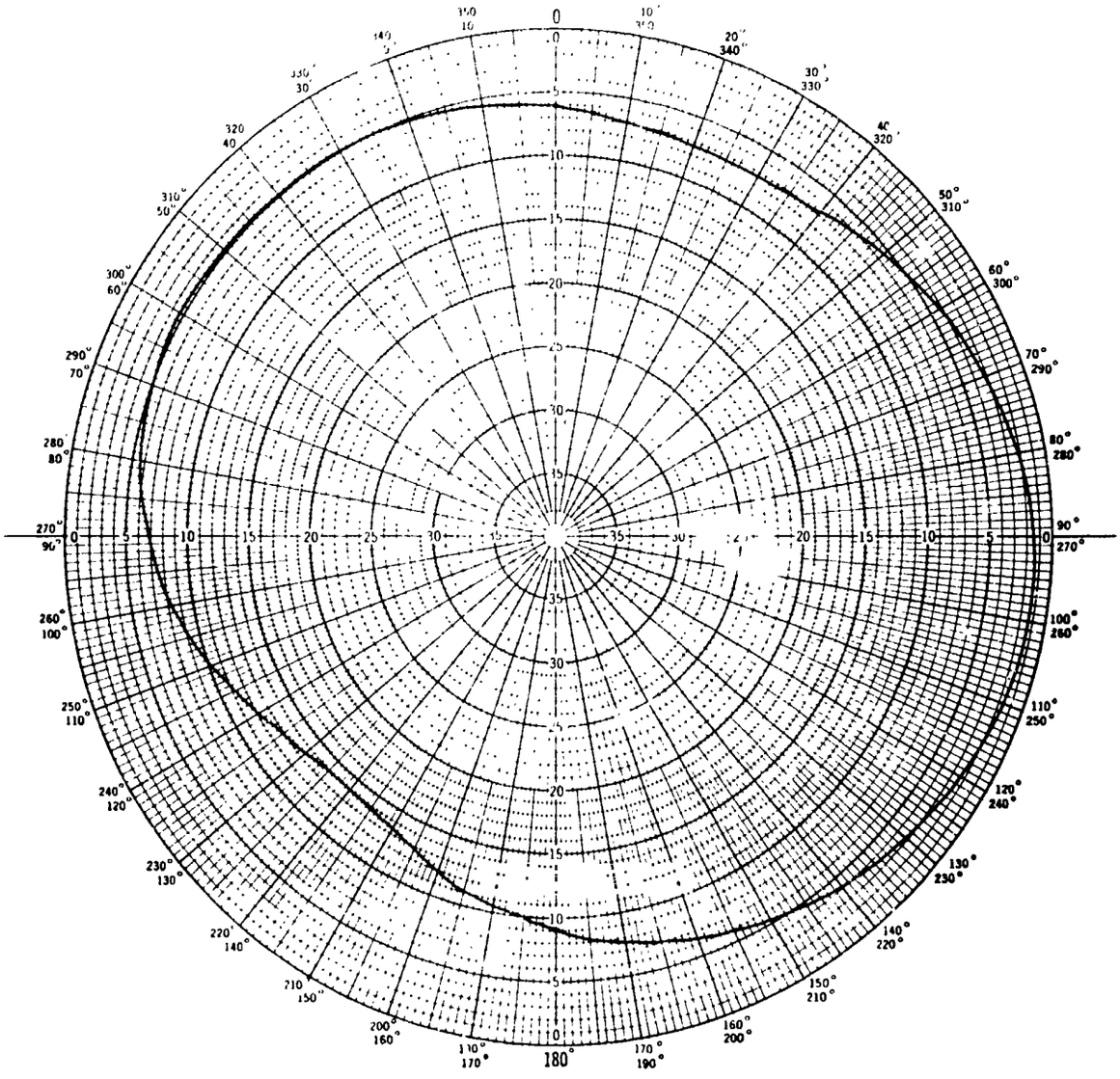

Fig. B-11. - A Conical Cut of the Antenna, $\theta = 60^{\circ}$